Experimental demonstration of Quantum Overlapping Tomography

Yang Zhengning,[1] Shihao Ru,[1,2] Lianzhen Cao,[3] Nikolay Zheludev,[1,4] and Weibo Gao[1,4,5,*]

[1] *Division of Physics and Applied Physics, School of Physical and Mathematical Sciences, Nanyang Technological University, Singapore 637371, Singapore*
[2] *School of Physics, Xi'an Jiaotong University, Xi'an 710049, China*
[3] *School of Physics and Photoelectric Engineering, Weifang University, Weifang 261061, China*
[4] *The Photonics Institute and Centre for Disruptive Photonic Technologies, Nanyang Technological University, Singapore 637371, Singapore*
[5] *Center for Quantum Technologies, National University of Singapore, Singapore 117543, Singapore*

(Dated: November 8, 2022)

Quantum tomography is one of the major challenges of large-scale quantum information research due to the exponential time complexity. In this work, we experimentally demonstrate quantum overlapping tomography [Phys. Rev. Lett. 124, 100401 (2020)], a scheme intent on characterizing critical information of a many-body quantum system in logarithmic time complexity. By comparing the measurement results of full state tomography and overlapping tomography, we show that overlapping tomography gives accurate information of the system with much fewer state measurements than full state tomography.

As more interest and effort have been put into the research of quantum information processing in recent years [1, 2], there have been remarkable advances in constructing and controlling large-scale quantum systems with a series of physical systems, including but not limited to superconducting circuits [3–5], linear optics [6, 7], ion trap [8, 9], and ultracold atoms [10]. Although it has been realistic to create and operate a large system with around 100 or even 1000 qubits [11, 12], it's still a question how to measure such many-body states and demonstrate the correlation between any two parts of the system. Due to the quantum nature of qubits, the information carried by a qubit cannot be read out with one single measurement [13]. Instead, one needs to perform multiple times of measurement with multiple sets of basis on one quantum state to reconstruct the density matrix representing the state [14]. As the number of qubits in the system goes up, the number of required measurements increases exponentially [15], leading to an unacceptable time complexity, which could overwhelm the stability of the system for even a moderate scale. In fact, for a system with just 10 qubits, a full state tomography (FST) has been considerably hard [16]. Driven by this challenge, various protocols have been raised to reduce the time complexity. Some protocols offer advantages for certain quantum states with special structures [17]. Some protocols can estimate an unknown state with higher efficiency, but they require quantum non-demolition measurement, which remains experimentally unavailable nowadays [18].

A more realistic idea is to retrieve limited but critical information by reconstructing the reduced density matrices of the small-scale subsystems of the huge-scale system, with much fewer measurements. Although this kind of 'partial' tomography doesn't give a full picture of the system, it is usually critical in application cases, such as the research on long-range order in many-body systems [19] and machine learning based on quantum neural networks [20]. However, even for this simplified task, the time complexity still can be unacceptable. Supposing we have a system of n qubits and hope to measure all the k-qubit subsystems, there are $\binom{n}{k}$ subsystems that need to be measured. For small k relative to n, we have $\binom{n}{k} \sim n^k$. Thus, the time complexity is $e^{O(k)} \times n^k$ because measuring each k-qubit subsystem has a time complexity $e^{O(k)}$. Even for a modest scale of $n = 50$ and $k = 2$, the total number of measurements will reach 10000N, where N stands for the required number of measurements to obtain a statistically significant result for each measurement setting. This number has been too much for a real experiment.

Quantum Overlapping Tomography (QOT) [21] is one

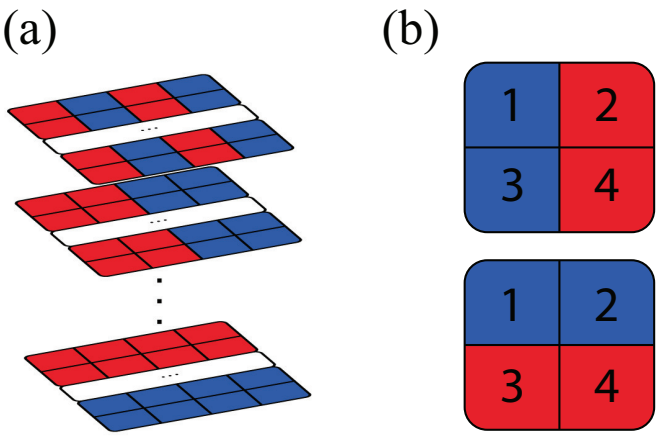

FIG. 1. (a) 2-qubit quantum overlapping tomography of a large-scale system. The whole system is divided into two groups, red and blue, in different strategies. For each dividing strategy, the two groups are measured on a different basis. (b) QOT dividing strategy for the $n = 4, k = 2$ case.

protocol proposed by J. Cotler and F. Wilczek, which makes use of the strong power of parallelism to simplify this task. With the overlapping nature of quantum many-body systems, QOT can reconstruct all $\binom{n}{k}$ k-qubit subsystems in logarithmic time complexity $\sim e^{O(k)} \log_k n$ by reorganizing the measurement dataset. With this scheme, for $n = 50$, $k = 2$, it's possible to reconstruct all the subsystems within less than 100N measurements, which means an over 100 times boost.

Due to its fascinating advantage, QOT has been attracting considerable attention from the community. Some researchers have started to use this method in their projects [22]. However, a general experimental scheme of QOT and the performance comparison between QOT and FST are still new topics to fill in. In this work, we experimentally demonstrate QOT on a 4-photon polarization entanglement system powered by spontaneous parametric down-conversion (SPDC). To apply the QOT scheme originating from exact tomography [23], which is not legitimate to use in experiments, into the experiment scenario, we develop an algorithm to perform a Bayesian mean estimation (BME) [24] to estimate the target states with the measurement dataset, for both FST and QOT. We compare the outcome of FST and QOT with a 4-photon GHZ state. To make the results comparable, the QOT estimation is performed with a subset of the measurement dataset that the FST uses, instead of a separate dataset. In addition, we generate a variation of GHZ state and show that QOT is capable to characterize general kinds of states.

In quantum information, any quantum state of a single qubit can be demonstrated with a two-dimension density matrix [23]

$$\hat{\rho} = \frac{1}{2}\sum_{i=0}^{3} S_i \hat{\sigma}_i, \hat{\sigma}_0 \equiv \begin{pmatrix} 1 & 0 \\ 0 & 1 \end{pmatrix}, \hat{\sigma}_1 \equiv \begin{pmatrix} 0 & 1 \\ 1 & 0 \end{pmatrix}, \hat{\sigma}_2 \equiv \begin{pmatrix} 0 & -i \\ i & 0 \end{pmatrix}, \hat{\sigma}_3 \equiv \begin{pmatrix} 1 & 0 \\ 0 & -1 \end{pmatrix} \quad (1)$$

S_i values can be given by $S_i = Tr\{\hat{\sigma}_i \hat{\rho}\}$, which indicates that it can be directly obtained with projective measurements.

Similarly, a general multi-qubit system with n qubits can be demonstrated with a density matrix with 2^n dimensions.

$$\hat{\rho} = \frac{1}{2^n} \sum_{i_1, i_2, \cdots, i_n = 0}^{3} S_{i_1, i_2, \cdots, i_n} \hat{\sigma}_{i_1} \otimes \hat{\sigma}_{i_2} \otimes \cdots \hat{\sigma}_{i_n} \quad (2)$$

To reconstruct the density matrix, the main task of a quantum full state tomography is to obtain all the $S_{i_1, i_2, \cdots, i_n}$ values. In theory, the values can be directly calculated with the results of measurement through exact tomography [23].

$$\begin{aligned} S_{i_1, i_2, \cdots, i_n} &= (\lambda_1 P_{\phi_{i_1}} + \lambda_1^{\perp} P_{\phi_{i_1}^{\perp}})(\lambda_2 P_{\phi_{i_2}} + \lambda_2^{\perp} P_{\phi_{i_2}^{\perp}}) \cdots (\lambda_n P_{\phi_{i_n}} + \lambda_n^{\perp} P_{\phi_{i_n}^{\perp}}) \\ &= (\lambda_1 \lambda_2 \cdots \lambda_n) P_{\phi_{i_1} \phi_{i_2} \cdots \phi_{i_n}} + (\lambda_1 \lambda_2 \cdots \lambda_n^{\perp}) P_{\phi_{i_1} \phi_{i_2} \cdots \phi_{i_n^{\perp}}} + \cdots + (\lambda_1^{\perp} \lambda_2^{\perp} \cdots \lambda_n^{\perp}) P_{\phi_{i_1^{\perp}} \phi_{i_2^{\perp}} \cdots \phi_{i_n^{\perp}}} \end{aligned} \quad (3)$$

Here we note ϕ_{i_j} as the eigenstate with eigenvalue $\lambda_j = 1$ and $\phi_{i_j}^{\perp}$ with eigenvalue $\lambda_j^{\perp} = -1$.$P_{\phi_{i_j}^{\perp}}$ stands for the probability. that j^{th} qubit is in $\phi_{i_j}^{\perp}$, which can be estimated with a finite number of measurements. For the case of $i_j = 0$, $\lambda_j P_{\phi_0} + \lambda_j^{\perp} P_{\phi_0^{\perp}} = 1$, which means this term would be "transparent" in the calculation.

For the whole system with n qubits, an array with $2n$ detectors is deployed to measure all 2^n eigenstates of element density matrix $\hat{\sigma}_{i_1} \otimes \hat{\sigma}_{i_2} \otimes \cdots \hat{\sigma}_{i_n}$ at the same time, with the measurement setting $\{i_1, i_2, \cdots, i_n\}$. In principle, 4^n settings are needed since each i_j has 4 possible values. However, for those settings with any $i_j = 0$, the $S_{i_1, i_2, \cdots, i_n}$ can be directly calculated with the measurement results by other settings with all $i_j = 0$. Thus, in practice, we need 3^n settings to reconstruct the density matrix of a system with n qubits.

Note that exact tomography is only usable with the assumption that the observed probabilities are theoretically perfect, which means the observation should be with no errors and be conducted through an infinite ensemble of states. In another word, Eq(3) is not valid for any real measurement, otherwise, it would lead to physically insufficient results. A common practice to reconstruct legitimate density matrices with real observation results is statistical estimation methods, such as Maximum Likelihood Estimation (MLE) [25] and Bayesian Mean Estimation (BME) [24, 26]. In this work, we develop an algorithm based on Gibbs sampling [27] to perform a Bayesian Mean Estimation with the measurement datasets for both FST and QOT.

Here we show how the QOT works in a $k = 2$ case. Firstly, we describe the task as reconstructing all $\binom{n}{k}$ 2-qubit reduced density matrices:

$$\hat{\rho}^{\{x_1, x_2\}} = \frac{1}{2^2} \sum_{i_1, i_2 = 0}^{3} S_{i_1, i_2}^{\{x_1, x_2\}} \hat{\sigma}_{i_1} \otimes \hat{\sigma}_{i_2} \quad (4)$$

where $\{x_1, x_2\}$ represents a 2-qubit subsystem of the n-qubit system. To obtain the values of $S_{i_1,i_2}^{\{x_1,x_2\}}$, Normally we need to pick all of the 2-qubit groups $\{x_1, x_2\}$ and measure them individually. For the n-qubit system, there are $\frac{n(n-1)}{2}$ of such subsystems, and $N \times 3^2 = 9N$ measurements need to be operated on each subsystem to get a tomography of them, which gives an $O(n^2)$ time complexity.

In QOT (Fig.1(a)) instead, we divide the n-qubit system into 2 groups, by $q = \lceil \log_2 n \rceil$ ways. The dividing strategy should satisfy the requirement that for any subsystem $\{x_1, x_2\}$, there is at least one divide where x_1 and x_2 are in different groups.

A dividing example of $n = 4$ case is given in (Fig.1(b)). The 4-qubit system $\{1, 2, 3, 4\}$, is divided in 2 different ways noted as $\{\{1, 2\}, \{3, 4\}\}$ and $\{\{1, 3\}, \{2, 4\}\}$. Then we measure the system in two steps:

1. Measure all the qubits in X,Y,Z basis respectively, which need $3N$ measurements in total.

2. For each divide out of the q divides, measure all qubits in group 1 in one basis $B_1 \in \{X, Y, Z\}$ and measure all qubits in group 2 in another different basis B_2. Thus, it takes 6 measurements for each of the q divides, which is a total of $6qN$.

So, we use $3+6q$ measurement basis sets in total, which gives a logarithmic time complexity. With an ideal probabilities dataset, density matrices $\hat{\rho}^{\{x_1,x_2\}}$ can be reconstructed by calculating the value

$$S_{i_1,i_2}^{\{x_1,x_2\}} = (\lambda_1 P_{\phi_{i_1}} + \lambda_1^{\perp} P_{\phi_{i_1}^{\perp}})(\lambda_2 P_{\phi_{i_2}} + \lambda_2^{\perp} P_{\phi_{i_2}^{\perp}}) \quad (5)$$

This calculation relies on the same assumption as exact tomography, so it is not valid for real measurements. Proper estimation is also necessary to reconstruct legitimate density matrices with the QOT dataset.

In our experiment, we build up a 4-qubit entangled system and try to reconstruct the 2-qubit subsystems of it [28]. If we operate FST on the 4-qubit system, we need $N \times 3^4 = 81N$ measurements for the task. For the subsystem reconstruction task that we have discussed, $N \times \binom{4}{2} \times 3^2 = 54N$ measurements are required. However, with QOT, only $N \times (3 + 6 \log_2 4) = 15N$ measurements are required to reconstruct all the 2-qubit subsystems.

Fig.2 shows an overview of the experimental set-up for generating and detecting a 4-photon GHZ state $\psi_{GHZ}^R = \frac{1}{\sqrt{2}}(|HVHV\rangle + e^{i\theta}|VHVH\rangle)$. Following Jones Calculus [33], the horizontal polarization $|H\rangle$ and vertical polarization $|V\rangle$ are defined as the eigenstates of Pauli matrix σ_z. $|L/R\rangle = \frac{1}{\sqrt{2}}(|H\rangle \pm i|V\rangle), |D/A\rangle = \frac{1}{\sqrt{2}}(|H\rangle \pm |V\rangle)$ are the eigenstates for σ_y and σ_x respectively. We use waveplates and polarization beamsplitters to measure qubits on a specific measurement basis. By detecting photons

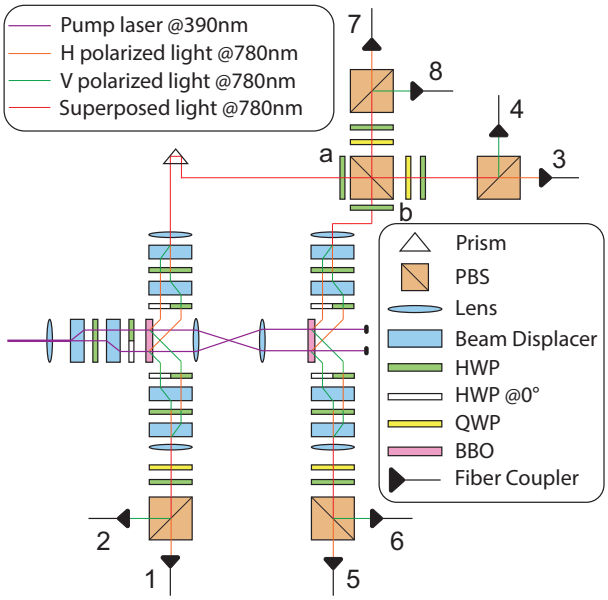

FIG. 2. Schematic of experimental set-up for generating 4-photon entanglement, with the detectors labeled by order. An ultrafast pulsed laser with the center wavelength of 390 nm, pulse duration of ∼100 fs, and repetition rate of 80 MHz was deployed to pump two sets of interference-based beam-like SPDC entanglement sources [29, 30]. The polarization-entangled photon pairs go through a post-selection interference to generate a 4-photon GHZ state, which is then measured by 8 single-photon detectors. To reduce the loss of two-fold fidelity caused by time-space correlation [31, 32], we applied narrow-band filters with λ_{FWHM}=3 nm and λ_{FWHM}=10 nm to the signal and idler photons respectively. The center wavelengths of both signal and idler photons are 780 nm. BBO: Barium Borate; PBS: polarization beam-splitter; HWP: half-wave plate; QWP: quarter-wave plate

in both output modes of PBS, we measure all 16 probabilities in parallel for one measurement basis set.

The two-fold coincidence counting rate can reach 100 kHz at pump power 550 mW, with a state fidelity $F > 0.97$. The singles count rates vary between 350 - 500 kHz with different channels, generating a 2-fold accidental rate around 2 kHz and a coincidence-to-accidental ratio (CAR) around 50:1. The 4-fold accidental rate is around 0.05 Hz. The single photon detecting efficiency is between $20 - 25\%$ with narrow-band filtering. We recorded 4-fold coincidences (for 16 sets of measurement basis spontaneously) for 300 s on each setting, with the total coincidence counting rate over 16 sets of basis around 10 Hz, with a CAR around 200:1. We performed an FST on this state to reconstruct the 4-qubit density matrix ρ^F. Comparing the tomography result with a given pure state $\rho^R = |\psi_{GHZ}^R\rangle\langle\psi_{GHZ}^R|$, the state fidelity $F^M = (Tr\sqrt{\sqrt{\rho^R}\rho^F\sqrt{\rho^R}})^2 = 0.922 \pm 0.013$.

For the QOT case, we focus on the 2-qubit subsystems of the 4-qubit entangled state. Thus, firstly, we obtain the density matrices of 2-qubit subsys-

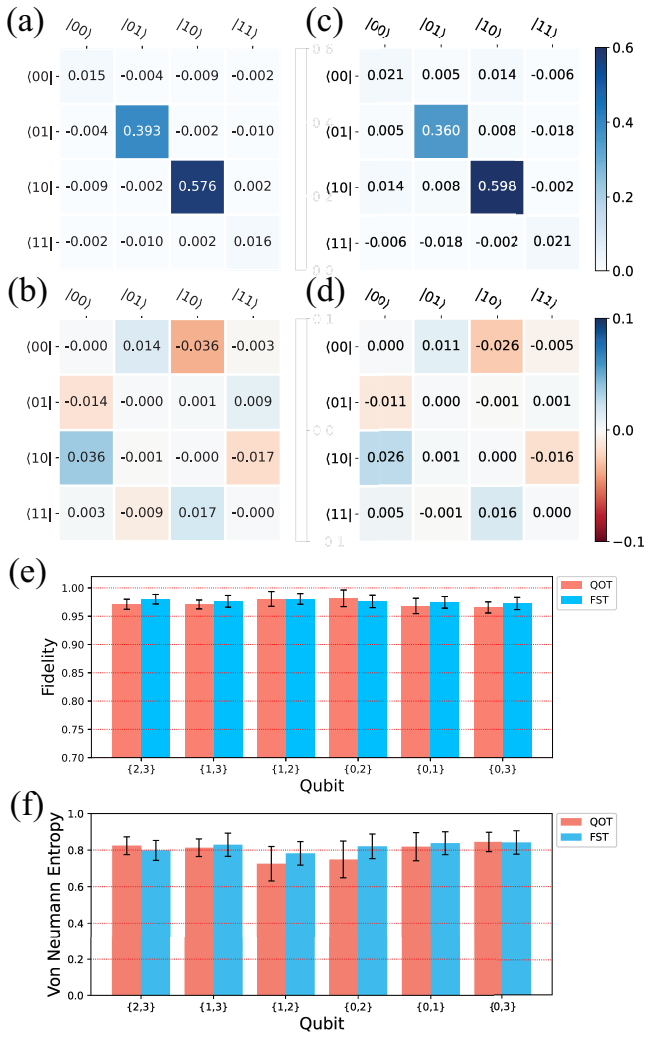

FIG. 3. (a) real and (b) imaginary part of density matrix of 2-qubit subsystem $\psi^F_{2,3}$ obtained by 4-qubit full state tomography (FST) (c) real and (d) imaginary part of density matrix of 2-qubit subsystem $\psi^O_{2,3}$ obtained by overlapping tomography. (e) 2-qubit state fidelities of $\psi^F_{i_1,i_2}/\psi^O_{i_1,i_2}$ with $(\psi^R_{GHZ})_{i_1,i_2}$ and (f) Von Newmann Entropy of subsystem $\psi^F_{i_1,i_2}$ and $\psi^O_{i_1,i_2}$. For (e-f), error bars show 95% confidence interval

tems $\rho^F_{j_1,j_2} = Tr_{i_1,i_2}\rho^M, i_1, i_2 \in \{1,2,3,4\}, \{j_1,j_2\} = \{1,2,3,4\}/\{i_1,i_2\}$ by calculating the partial trace. Then we perform overlapping tomography on the same state, reconstructing the density matrices $\rho^O_{i_1,i_2}$ of 2-qubit subsystems. By comparing $\rho^F_{i_1,i_2}$ and $\rho^O_{i_1,i_2}$ in density matrix visualization (Fig.3(a-d)) and state fidelity (Fig.3(e)), we confirmed that QOT gives highly similar results to the outcome from 4-qubit FST. The fidelity differences are less than 0.01 within the margin of error, which displays the similarities between density matrices estimated with QOT and 4-qubit FST.

To further characterize the states in this case, we calculated and compared the Von Neumann Entropy (VNE) [34] $S = -Tr(\rho \cdot \ln \rho)$ of $\rho^F_{i_1,i_2}$ and $\rho^O_{i_1,i_2}$. For the 2-qubit

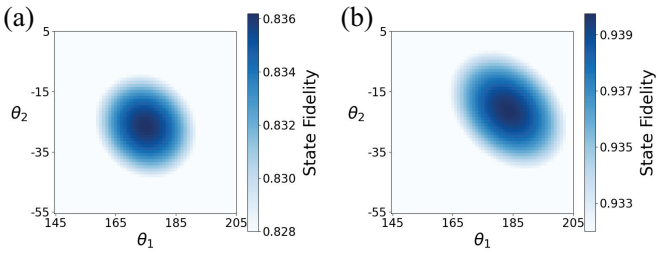

FIG. 4. (a) State fidelity $F(\theta_1,\theta_2)$ between 4-qubit state ψ'^F reconstructed via 4-qubit FST and reference state $\psi'^R(\theta_1,\theta_2)$, F reached peak at $\theta_1 = 175°, \theta_2 = -27°$. (b) State fidelity $F_{0,2}(\theta_1,\theta_2)$ between 2-qubit subsystem $\psi'_{0,2}$ reconstructed via overlapping tomography and reduced reference state $\psi'^R_{0,2}(\theta_1,\theta_2)$. $F_{0,2}$ reached peak at $\theta_1 = 183°, \theta_2 = -21°$.

subsystems of an ideal 4-qubit GHZ state, the quantum state should be a mixed state consisting of two maximally entangled Bell states $|\Psi\rangle$, and the VNE should be $S \approx ln2 = 0.69$. State or measurement error usually increases this value, which indicates the state is more 'mixed' and less 'entangled'. By comparing VNE $S^O_{i_1,i_2}$ and $S^O_{i_1,i_2}$ (Fig.3(f)), we find that overlapping tomography gives overall similar results with the 4-qubit FST. Though all differences between VNE results given by QOT and 4-qubit FST are within the margin of error, for some subsystems, the VNE by QOT are visibly smaller than that by FST. This may be due to the QOT results being estimated with fewer sets of measurement data than the 4-qubit FST, which reduces the influence of inconsistency of measurements originating from environment vibration and imperfect experiment operations.

Further, we use overlapping tomography to characterize an alternative state ψ'. The reference state wavefunction for this case is $\psi'^R = \frac{1}{\sqrt{2}}(|D'VD''V\rangle + e^{i(\theta_1+\theta_2)}|A'HA''H\rangle)$, where $|D'\rangle = |H\rangle + e^{i\theta_1}|V\rangle, |A'\rangle = |H\rangle - e^{i\theta_1}|V\rangle, |D''\rangle = |H\rangle + e^{i\theta_2}|V\rangle, |A''\rangle = |H\rangle - e^{i\theta_2}|V\rangle$. We generated this state by setting HWP a and b in Fig.2 to $\theta_a = -22.5°$ and $\theta_b = -22.5°$. Similarly, we compare the result of 4-qubit FST and QOT with density matrices visualization [28]. This result shows QOT is equally efficient for different multi-qubit states, indicating that QOT is a promising method to characterize common quantum states.

In the wavefunction of ψ'^R, θ_1 and θ_2 are extra phases introduced by the SPDC process, which can be estimated by calculating the fidelity between the measurement result and reference states. We estimated $\theta_1 = 175°, \theta_2 = -21°$ by comparing the 4-qubit density matrix ρ'^F obtained by 4-qubit FST with reference state $\rho'^R(\theta_1,\theta_2) = |\psi'^R(\theta_1,\theta_2)\rangle\langle\psi'^R(\theta_1,\theta_2)|$ (Fig.4(a)). We also use the subsystems reconstructed via QOT to estimate the state phase θ_1, θ_2 by comparing the density matrices $\rho'^O_{i_1,i_2}$ with reference state $\rho'^R_{i_1,i_2}(\theta_1\theta_2)$ (Fig.4(b)). Though a difference exists between the two estimations,

considering the small derivative of fidelity to both θs, the results are reasonably close with each other as the difference between two estimations corresponds to less than 0.8% difference in state fidelity. Besides, since QOT takes fewer measurements, system inconsistency affects QOT less than FST, which may also contribute to the difference. This feature could be a significant advantage when measuring large systems. This result shows that QOT can be used to extract important state parameters with a significantly reduced time complexity too.

To give a further demonstration of the advantage of QOT, we perform QOT on a linear optical six-qubit system [28]. In such a system, we managed to observe six-photon coincidence events with a count rate of 0.05 Hz. To perform a six-qubit FST, the state needs to be measured in 729 sets of basis. As 700 events are recorded for each basis sets to get a reasonable witness, the whole FST would take around 120 days, which is unacceptable given the stability of optical set-ups. By contrast, with QOT, we can reconstruct all 15 2-qubit subsystems with only 21 sets of basis and the measurement only take around 80 hours.

In summary, we performed quantum overlapping tomography to characterize 4-qubit GHZ states. By comparing the QOT results with FST results, we showed that QOT is capable to reconstruct subsystems with a given scale and extract important parameters of a 4-qubit state, with a remarkably reduced number of measurements. This scheme is directly applicable to quantum states with a wider range of structures and larger scale, which could be significant for the future development of quantum information.

We acknowledge Singapore National Research foundation through QEP grant (NRF2021-QEP2-01-P02, NRF2021-QEP2-03-P01, 2019-0643 (QEP-P2) and 2019-1321 (QEP-P3)) and Singapore Ministry of Education (MOE2016-T3-1-006 (S)).

* wbgao@ntu.edu.sg

[1] T. D. Ladd, F. Jelezko, R. Laflamme, Y. Nakamura, C. Monroe, and J. L. O'Brien, Quantum computers, Nature **464**, 45 (2010).

[2] M. A. Nielsen and I. Chuang, Quantum computation and quantum information (2002).

[3] M. H. Devoret and R. J. Schoelkopf, Superconducting circuits for quantum information: An outlook, Science **339**, 1169 (2013).

[4] F. Arute, K. Arya, R. Babbush, D. Bacon, J. C. Bardin, R. Barends, R. Biswas, S. Boixo, F. G. S. L. Brandao, D. A. Buell, B. Burkett, Y. Chen, Z. Chen, B. Chiaro, R. Collins, W. Courtney, A. Dunsworth, E. Farhi, B. Foxen, A. Fowler, C. Gidney, M. Giustina, R. Graff, K. Guerin, S. Habegger, M. P. Harrigan, M. J. Hartmann, A. Ho, M. Hoffmann, T. Huang, T. S. Humble, S. V. Isakov, E. Jeffrey, Z. Jiang, D. Kafri, K. Kechedzhi, J. Kelly, P. V. Klimov, S. Knysh, A. Korotkov, F. Kostritsa, D. Landhuis, M. Lindmark, E. Lucero, D. Lyakh, S. Mandrà, J. R. McClean, M. McEwen, A. Megrant, X. Mi, K. Michielsen, M. Mohseni, J. Mutus, O. Naaman, M. Neeley, C. Neill, M. Y. Niu, E. Ostby, A. Petukhov, J. C. Platt, C. Quintana, E. G. Rieffel, P. Roushan, N. C. Rubin, D. Sank, K. J. Satzinger, V. Smelyanskiy, K. J. Sung, M. D. Trevithick, A. Vainsencher, B. Villalonga, T. White, Z. J. Yao, P. Yeh, A. Zalcman, H. Neven, and J. M. Martinis, Quantum supremacy using a programmable superconducting processor, Nature **574**, 505 (2019).

[5] Y. Wu, W.-S. Bao, S. Cao, F. Chen, M.-C. Chen, X. Chen, T.-H. Chung, H. Deng, Y. Du, D. Fan, M. Gong, C. Guo, C. Guo, S. Guo, L. Han, L. Hong, H.-L. Huang, Y.-H. Huo, L. Li, N. Li, S. Li, Y. Li, F. Liang, C. Lin, J. Lin, H. Qian, D. Qiao, H. Rong, H. Su, L. Sun, L. Wang, S. Wang, D. Wu, Y. Xu, K. Yan, W. Yang, Y. Yang, Y. Ye, J. Yin, C. Ying, J. Yu, C. Zha, C. Zhang, H. Zhang, K. Zhang, Y. Zhang, H. Zhao, Y. Zhao, L. Zhou, Q. Zhu, C.-Y. Lu, C.-Z. Peng, X. Zhu, and J.-W. Pan, Strong quantum computational advantage using a superconducting quantum processor, Phys. Rev. Lett. **127**, 180501 (2021).

[6] H.-S. Zhong, Y.-H. Deng, J. Qin, H. Wang, M.-C. Chen, L.-C. Peng, Y.-H. Luo, D. Wu, S.-Q. Gong, H. Su, Y. Hu, P. Hu, X.-Y. Yang, W.-J. Zhang, H. Li, Y. Li, X. Jiang, L. Gan, G. Yang, L. You, Z. Wang, L. Li, N.-L. Liu, J. J. Renema, C.-Y. Lu, and J.-W. Pan, Phase-programmable gaussian boson sampling using stimulated squeezed light, Phys. Rev. Lett. **127**, 180502 (2021).

[7] P. Kok, W. J. Munro, K. Nemoto, T. C. Ralph, J. P. Dowling, and G. J. Milburn, Linear optical quantum computing with photonic qubits, Rev. Mod. Phys. **79**, 135 (2007).

[8] C. Monroe and J. Kim, Scaling the ion trap quantum processor, Science **339**, 1164 (2013).

[9] C. Figgatt, A. Ostrander, N. M. Linke, K. A. Landsman, D. Zhu, D. Maslov, and C. Monroe, Parallel entangling operations on a universal ion-trap quantum computer, Nature **572**, 368 (2019).

[10] M. Saffman, T. G. Walker, and K. Mølmer, Quantum information with rydberg atoms, Rev. Mod. Phys. **82**, 2313 (2010).

[11] B. Yang, H. Sun, R. Ott, H.-Y. Wang, T. V. Zache, J. C. Halimeh, Z.-S. Yuan, P. Hauke, and J.-W. Pan, Observation of gauge invariance in a 71-site bose–hubbard quantum simulator, Nature **587**, 392 (2020).

[12] B. Yang, H. Sun, C.-J. Huang, H.-Y. Wang, Y. Deng, H.-N. Dai, Z.-S. Yuan, and J.-W. Pan, Cooling and entangling ultracold atoms in optical lattices, Science **369**, 550 (2020).

[13] K. Kraus, A. Böhm, J. Dollard, and W. Wootters, States, effects, and operations: Fundamental notions of quantum theory (1983).

[14] G. M. D'Ariano and P. Lo Presti, Quantum tomography for measuring experimentally the matrix elements of an arbitrary quantum operation, Phys. Rev. Lett. **86**, 4195 (2001).

[15] R. O'Donnell and J. Wright, Efficient quantum tomography, Proceedings of the forty-eighth annual ACM symposium on Theory of Computing , 899 (2016).

[16] C. Song, K. Xu, W. Liu, C.-p. Yang, S.-B. Zheng, H. Deng, Q. Xie, K. Huang, Q. Guo, L. Zhang, P. Zhang,

D. Xu, D. Zheng, X. Zhu, H. Wang, Y.-A. Chen, C.-Y. Lu, S. Han, and J.-W. Pan, 10-qubit entanglement and parallel logic operations with a superconducting circuit, Phys. Rev. Lett. **119**, 180511 (2017).
[17] B. P. Lanyon, C. Maier, M. Holzäpfel, T. Baumgratz, C. Hempel, P. Jurcevic, I. Dhand, A. S. Buyskikh, A. J. Daley, M. Cramer, M. B. Plenio, R. Blatt, and C. F. Roos, Efficient tomography of a quantum many-body system, Nature Physics **13**, 1158 (2017).
[18] S. Aaronson, Shadow tomography of quantum states, SIAM Journal on Computing **49**, STOC18 (2020).
[19] U. Schollwöck, The density-matrix renormalization group, Rev. Mod. Phys. **77**, 259 (2005).
[20] M. Schuld, I. Sinayskiy, and F. Petruccione, The quest for a quantum neural network, Quantum Information Processing **13**, 2567 (2014).
[21] J. Cotler and F. Wilczek, Quantum overlapping tomography, Phys. Rev. Lett. **124**, 100401 (2020).
[22] F. B. Maciejewski, F. Baccari, Z. Zimborás, and M. Oszmaniec, Modeling and mitigation of cross-talk effects in readout noise with applications to the Quantum Approximate Optimization Algorithm, Quantum **5**, 464 (2021).
[23] J. Altepeter, E. Jeffrey, and P. Kwiat, Photonic state tomography (Academic Press, 2005) pp. 105–159.
[24] R. Blume-Kohout, Optimal, reliable estimation of quantum states, New Journal of Physics **12**, 043034 (2010).
[25] K. Banaszek, G. M. D'Ariano, M. G. A. Paris, and M. F. Sacchi, Maximum-likelihood estimation of the density matrix, Phys. Rev. A **61**, 010304(R) (1999).
[26] J. M. Lukens, K. J. H. Law, A. Jasra, and P. Lougovski, A practical and efficient approach for bayesian quantum state estimation, New Journal of Physics **22**, 063038 (2020).
[27] S. Geman and D. Geman, Stochastic relaxation, gibbs distributions, and the bayesian restoration of images, IEEE Transactions on Pattern Analysis and Machine Intelligence **PAMI-6**, 721 (1984).
[28] See Supplemental Information Sec. I-IV for detailed experimental methods, Sec. V for full results of 4-qubit experiments, and Sec. VI for results of 6-qubit QOT experiment.
[29] H.-S. Zhong, Y. Li, W. Li, L.-C. Peng, Z.-E. Su, Y. Hu, Y.-M. He, X. Ding, W. Zhang, H. Li, L. Zhang, Z. Wang, L. You, X.-L. Wang, X. Jiang, L. Li, Y.-A. Chen, N.-L. Liu, C.-Y. Lu, and J.-W. Pan, 12-photon entanglement and scalable scattershot boson sampling with optimal entangled-photon pairs from parametric down-conversion, Phys. Rev. Lett. **121**, 250505 (2018).
[30] P. G. Kwiat, K. Mattle, H. Weinfurter, A. Zeilinger, A. V. Sergienko, and Y. Shih, New high-intensity source of polarization-entangled photon pairs, Phys. Rev. Lett. **75**, 4337 (1995).
[31] W. P. Grice, A. B. U'Ren, and I. A. Walmsley, Eliminating frequency and space-time correlations in multiphoton states, Phys. Rev. A **64**, 063815 (2001).
[32] X.-L. Wang, L.-K. Chen, W. Li, H.-L. Huang, C. Liu, C. Chen, Y.-H. Luo, Z.-E. Su, D. Wu, Z.-D. Li, H. Lu, Y. Hu, X. Jiang, C.-Z. Peng, L. Li, N.-L. Liu, Y.-A. Chen, C.-Y. Lu, and J.-W. Pan, Experimental ten-photon entanglement, Phys. Rev. Lett. **117**, 210502 (2016).
[33] R. C. Jones, A new calculus for the treatment of optical systemsi. description and discussion of the calculus, J. Opt. Soc. Am. **31**, 488 (1941).
[34] P. Calabrese and J. Cardy, Entanglement entropy and quantum field theory, Journal of Statistical Mechanics: Theory and Experiment **2004**, P06002 (2004).